IEEE Access
Multidisciplinary | Rapid Review | Open Access Journal

Received June 19, 2018, accepted August 4, 2018, date of publication August 20, 2018, date of current version September 7, 2018.

Digital Object Identifier 10.1109/ACCESS.2018.2866094

Real-Time Maximum Spectral Efficiency for Massive MIMO and Its Limits

WAEL BOUKLEY HASAN, (Student Member, IEEE), PAUL HARRIS, (Student Member, IEEE), ANGELA DOUFEXI, (Member, IEEE), AND MARK BEACH, (Member, IEEE)
Communication Systems and Networks Group, University of Bristol, Bristol BS8 1UB, U.K.

Corresponding author: Wael Boukley Hasan (wb14488@bristol.ac.uk)

The authors wish to thank Bristol City Council for access to the hardware facility and the financial support from the EPSRC (CDT in Communications, EP/I028153/1) and BBC R&D.

ABSTRACT This paper evaluates the impact of spatially multiplexing an increasing number of users within a single-cell massive multiple-input, multiple-output (MIMO) system. The highest spectral efficiency (SE) of 145.6 bits/s/Hz achieved for any wireless system to date and its limitation factors are presented. Recent works on massive MIMO show that there is a peak value for sum SE achieved by serving a certain number of users. It was shown that until the sum SE reached its peak value, the maximum sum SE is achieved by serving all users simultaneously. These results were based on perfect channel state information (CSI), Shannon capacity calculations, or using a very large number of antennas at the base station (BS). As opposed to the aforementioned results, we show that the maximum sum SE with practical number of antennas could be achieved by decreasing the number of users from the maximum before the sum SE reached its peak value, through an optimization of the modulation scheme. This is done by calculating the sum SE based on the error vector magnitude (EVM) performance and extrapolating this to match the EVM requirements of candidate modulation formats. The impact of uplink (UL) CSI accuracy on the downlink (DL) data transmission is also introduced, showing the heightened sensitivity that it has to inaccurate CSI mapping due to hardware imbalance between UL and DL transmissions. It is also shown that hardware with high quality could be better than increasing the number of antennas at the BS. All the aforementioned points are validated with experimental results obtained from a massive MIMO testbed.

INDEX TERMS CSI, EVM, massive MIMO, 5G, spectral efficiency, testbed, validation.

I. INTRODUCTION

Massive MIMO is a multi-user (MU) MIMO system with a large number of antennas at the BS serving several users within the same time and frequency resource [1]. Despite promising theoretical results that can be found well documented in [1] and [2], massive MIMO introduces many new, challenging problems when it comes to a real-time system implementation. Field trials such as those recently conducted by ZTE [3], Huawei [4] and Facebook [5] support the trend towards using this technology in future 5G wireless systems. The theoretical results in [1] show that significant capacity improvements are possible in MU MIMO by increasing the number of antenna elements at the BS. The ''channel hardening'' synonymous with massive MIMO [6] was observed in the field trials documented in [7]–[9]. In theory, the user channel vectors become pairwise orthogonal as the number of BS antennas is increased, facilitating the effective use of matched filtering (MF) [10]. The user-side channel Gram matrix from the field trials in [8] and [9] indicates the level of spatial orthogonality achieved when using a practical number of antennas may not be ideal. When the user channels become more correlated, it is likely that zero-forcing (ZF) or Minimum Mean Square Error (MMSE) will be required for reliable data transmission.

Accurate CSI is crucial for correct MU MIMO operation [1]. Several pieces of research have investigated the effect of inaccurate CSI in massive MIMO. The work in [11] illustrates the impact of hardware impairments for the DL of a single cell with different channel conditions. It shows how the number of BS antenna elements and their spacings can affect the Error Vector Magnitude (EVM) at the user equipment (UE) side. The hardware impairment impact for a single-cell scenario was addressed in [12]. The paper shows how the number of antennas affects the average sum rate with different channel models. The effect of imperfect channel reciprocity and CSI error was also covered in [13] for DL transmissions.

The paper introduced a model that considers the impact of RF mismatches on the linear precoding for a time division duplex (TDD) massive MIMO system. The relationship between the output signal to interference plus noise ratio (SINR) and the amplitude error variance were illustrated for ZF and MF. The impact of inaccurate CSI in a single-cell for both UL and DL was covered in [14]. The impact of non-ideal hardware on the capacity limits was covered in [15] for both UL and DL in a multi-cell scenario. It shows how the pilot length and the number of antennas at the BS are affected by the relative estimation error per antenna. The multi-cell scenario was then covered in [16] for both UL and DL. It shows how the number of antennas, pilot allocation and hardware impairments affects the spectral efficiency.

Although some research has investigated the impact of inaccurate CSI in massive MIMO performance, some topics need further investigation. Firstly, the approaches used to calculate the sum SE are based on Shannon capacity calculations and by using a very large number of antennas at the BS. These approaches show that there is a peak value for sum SE achieved by serving a certain number of users. And until the sum SE reaches its peak value, the maximum sum SE is achieved by serving all users simultaneously. However in a real-time massive MIMO system, these approaches are not applicable and do not consider using different modulation and coding scheme (MCS) orders. Secondly, most of the imperfect channel reciprocity work assumes accurate UL CSI which can't be acquired in reality. Thirdly, most available results are based on independent and identically distributed (IID) channels and do not cover SE comparison between different decoders/precoders for UL and DL data transmission with a practical number of antennas at the BS. Lastly, there is no publicly available work on experientially validating the impact of inaccurate CSI on massive MIMO performance. As the theoretical work proposed that increasing number of antennas at the BS decreases the interference caused by inaccurate CSI and from the channel itself, no validation has been published. Several massive MIMO trials have conducted as a proof of concept. Thus, the need for validation is high, as the industry needs to fully understand the trade-off between number of antennas (cost) and system performance.

A. MAIN CONTRIBUTIONS OF THE PAPER

Below, we summarize the main contributions of this work.

- We present per-cell SE of 145.6 bit/s/Hz achieved by a mean of a 128-antenna massive MIMO testbed. We also introduce the challenges and the limiting factors we faced when increasing the SE value in that trial.
- We show that the sum SE should be calculated based on the EVM performance instead of using Shannon capacity calculations for realistic performance. As opposed to the results obtained using Shannon capacity, we show that the maximum sum SE with practical number of antennas could be achieved by decreasing the number of users before the sum SE reached its peak value.
- We show that the inaccurate UL CSI has greater impact on the DL data transmission than it has on the UL data transmission due to the error amplification caused by the reciprocity calibration matrix.
- We show that by using ZF or MMSE, a lower number of antennas at the BS with high hardware quality could be better than increasing the number of antennas and reducing the hardware quality.
- We validate all the above points experimentally with real-time results using a software-defined radio massive MIMO testbed.

B. NOTATION

Boldface (lower case) is used for column vectors, $\boldsymbol{x}$, and (upper case) for matrices, $\boldsymbol{X}$. The operators $(.)^T$ and $(.)^H$ denote transpose and Hermitian transpose. The element in the nth row and mth column of matrix $\boldsymbol{A}$ is denoted by $(A)_{n,m}$. The operator $\mathbb{E}\{.\}$ denotes the expected value. $\Re\{.\}$ and $\Im\{.\}$ return the real and imaginary part of their arguments. The matrix $\boldsymbol{I}$ denotes the identity matrix, and $diag\{a_1, a_2, \ldots a_M\}$ denotes an $M \times M$ diagonal matrix with diagonal entries given by $a_1, a_2, \ldots, a_M$. The set of the complex numbers and the set containing zero and the real positive numbers are denoted by $\mathbb{C}$ and $\mathbb{R}$, respectively.

C. PAPER OUTLINE

The remaining sections of the paper are as follows. Section II presents the highest spectral efficiency achieved for any wireless system to date and introduces the challenges and the limiting factors. Section III presents the system models. Section IV shows the impact of adding more users on massive MIMO performance with inaccurate CSI in UL data transmission by using MF, ZF and MMSE. Section V shows how the reciprocity calibration error is affected by the UL CSI accuracy and the impact of adding more users in DL data transmission. Section VI shows the difference between using Shannon capacity calculations and the EVM performance on maximizing the sum SE with IID and real-channels. Section VII provides a comparison between adding more antennas at the BS and building hardware with better quality. Section VIII validates all the points raised in sections IV, V, VI and VII experimentally. Lastly, Section IX summarizes the key results from this work.

II. SERVING 22 USERS IN REAL-TIME WITH MASSIVE MIMO AND ITS LIMITS

A. MEASUREMENT ENVIRONMENT

The upper level of the Merchant Venturers Building atrium at the University of Bristol was used as the test environment with a patch panel antenna array to serve 22 user clients placed 24.8m away on the opposite balcony. The array was setup in a 4×32 configuration with alternate H & V polarizations for all 128 antennas. The UEs were in line-of-sight (LOS) and placed in a straight line with 2.5 wavelength spacing at a 3.51 GHz carrier frequency. However, this

Fig. 1. Measurement trial with the UEs 24.8m away.

environment was not completely static, as it was a normal working day with students and staff present. An overview of the setup can be seen in Fig. 1.

B. SYSTEM CONFIGURATION

The frame schedule was configured such that channel estimation was performed in 5ms intervals, and all remaining slots were assigned for UL data with a 256-quadrature amplitude modulation (QAM) MCS. ZF detection was used for all throughput measurements and equal transmit power was applied for all UEs. 100 channel data captures were recorded to disk at an interval of approximately 200ms, resulting in a total measurement period of approximately 3 minutes. Detailed information about MIMO processing, frame schedule, synchronization and channel processing are available in [8].

C. OUTCOMES AND LIMITATIONS

In real-time it was possible to connect 22 users with 256-QAM and obtain the decoded UL constellations shown in Fig. 2 using 128 bit complex floating point processing. The absolute throughput could not be measured for 22 users as only decimated host detection was performed, but by observing the clarity of the constellations and the degree of spatial orthogonality achieved, an appropriate estimation could be made. 22 UEs were successfully served, which would equate to 145.6 bits/s/Hz using the frame schedule in [8]. This is a record reported result for spectral efficiency [17] and truly demonstrates the tremendous potential of massive MIMO technology for improving system throughput without bandwidth expansion.

Connecting a 23^{rd} user caused significant degradation in the constellation quality and the physical location of this additional user within the line of 24 UEs (see Fig. 1) had no impact. Therefore, it is believed this could be related to CSI accuracy introduced in [14]. Further analysis through trials and simulations is now provided in this paper to investigate the impact of inaccurate CSI and number of UEs on massive MIMO performance.

III. SYSTEM MODEL

A single-cell Massive-MIMO architecture is considered in this work. The base station is equipped with a large number of antennas (M) and serves a number of active single-antenna

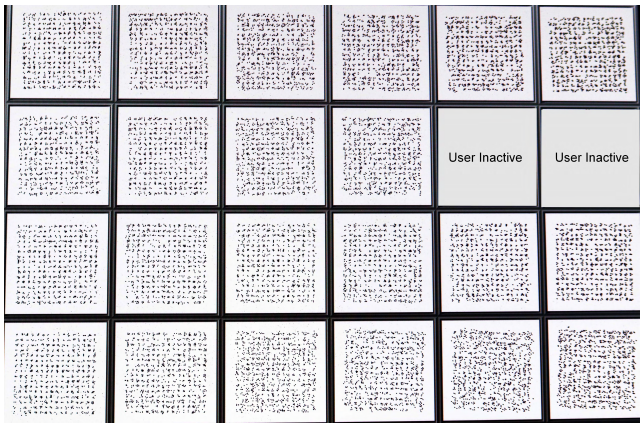

Fig. 2. 256-QAM UL constellations from 22 UEs in trial two: 24.8m with 50cm client separation.

users (K) where ($M \gg K$). The system operates in TDD mode and uses the same time-frequency resources for all users. Each UE transmits a frequency-orthogonal UL pilot for the channel estimation. The estimated UL channel matrix between the UEs and the BS is denoted by $\hat{\boldsymbol{H}}_{ul} \in \mathbb{C}^{M\times K}$. While the actual UL channel matrix during the uplink data transmission is denoted by $\boldsymbol{H}_{ul} \in \mathbb{C}^{M\times K}$, which is given by

$$\boldsymbol{H}_{ul} = \hat{\boldsymbol{H}}_{ul} + \boldsymbol{E}_{ul} \tag{1}$$

where $\boldsymbol{E}_{ul} \in \mathbb{C}^{M\times K}$ is the difference between the estimated channel and the actual channel during the uplink data transmission. This error could be caused by hardware impairments, interpolation across frequency, large-scale channel attenuation and any other potential sources. In this paper the error in the UL channel estimation between the UE and the BS is modeled as a complex Gaussian distribution $\sim \mathcal{CN}\left(\mathbf{0}, \sigma_e^2 \boldsymbol{I}_M\right)$, where $\boldsymbol{I}_M$ is the $M \times M$ identity matrix and σ_e^2 is the error variance [18]. Whilst this model could not be so accurate in reality, it serves to illustrate the potential effects of UL CSI inaccuracies in massive MIMO. The equalized UL signal $\hat{\boldsymbol{x}} \in \mathbb{C}^{\mathbb{K}}$ can be expressed as

$$\hat{\boldsymbol{x}} = \boldsymbol{W}\left(\sqrt{\rho_{ul}}\boldsymbol{H}_{ul}\boldsymbol{x} + \boldsymbol{n}\right) \tag{2}$$

where x represents the transmitted symbol vector from all users in the same cell, normalized as $\mathbb{E}\left\{|x_k|^2\right\} = 1$. The corresponding UL transmit power is denoted by ρ_{ul}. Simple UL power control is assumed in this paper. The UL transmit power is adjusted so the received signal to noise ratio (SNR) from all users is the same. The additive noise vector in UL is denoted by $\boldsymbol{n}$. The noise variance from the antennas at the BS is modeled as $\sim \mathcal{CN}\left(\mathbf{0}, \sigma_n^2 \boldsymbol{I}_M\right)$, where σ_n^2 is the noise variance. $\boldsymbol{W} \in \mathbb{C}^{K\times M}$is the linear decoder matrix, formed by using MMSE, ZF or MF.

While it is generally agreed that the propagation channel is reciprocal [19], the transceiver radio frequency (RF) chains at both ends of the link are generally not [20]. Therefore, the actual DL channel matrix during the DL data transmission is denoted by $\boldsymbol{H}_{dl} \in \mathbb{C}^{K\times M}$. The estimated DL channel matrix

$\hat{\boldsymbol{H}}_{dl} \in \mathbb{C}^{\mathrm{K}\times\mathrm{M}}$ and how it is affected by $\hat{\boldsymbol{H}}_{ul}$ are covered in section V. The received downlink signal can be written as

$$\boldsymbol{y}_{dl} = \sqrt{\rho_{dl}}\boldsymbol{H}_{dl}\boldsymbol{P}\boldsymbol{s} + \boldsymbol{d} \tag{3}$$

where s represents the transmitted symbol vector from the BS to users in the same cell, normalized as $\mathbb{E}\left\{|s_k|^2\right\} = 1$. The corresponding DL transmit power is denoted by ρ_{dl}. $\boldsymbol{P} \in \mathbb{C}^{\mathrm{M}\times\mathrm{K}}$ is the linear precoder matrix, formed by using MMSE, ZF or MF. d is the additive noise vector in DL. The noise variance from the users' antenna is modeled as $\sim \mathcal{CN}\left(\boldsymbol{0}, \sigma_d^2\boldsymbol{I}_K\right)$, where σ_d^2 is the noise variance.

IV. ACCUMULATIVE ERROR AMPLIFICATION IN UL

With imperfect channel estimation the error in equation 1 will always be added to the estimated channel. In sections A, B and C below, the impact of adding users with inaccurate CSI is explained for MF and ZF in the UL. From (2), the equalized signal vector can be written as follows:

$$\begin{aligned}\hat{\boldsymbol{x}} &= \sqrt{\rho_{ul}}\boldsymbol{W}\boldsymbol{H}_{ul}\boldsymbol{x} + \boldsymbol{W}\boldsymbol{n} \\ &= \sqrt{\rho_{ul}}\left(\boldsymbol{W}\boldsymbol{E}_{ul} + \boldsymbol{W}\hat{\boldsymbol{H}}_{ul}\right)\boldsymbol{x} + \boldsymbol{W}\boldsymbol{n} \\ &= \sqrt{\rho_{ul}}\boldsymbol{W}\boldsymbol{E}_{ul}\boldsymbol{x} + \sqrt{\rho_{ul}}\boldsymbol{W}\hat{\boldsymbol{H}}_{ul}\boldsymbol{x} + \boldsymbol{W}\boldsymbol{n}\end{aligned} \tag{4}$$

The number of users affect the actual equalized signal for the target user k. This can be shown by rearranging (4) as follows

$$\hat{\boldsymbol{x}}_k = \underbrace{\sqrt{\rho_{ul_k}}\sum_{i=1}^{K}(\boldsymbol{W}\boldsymbol{E}_{ul})_{k,i}\boldsymbol{x}_i}_{\text{Cumulative Error}} + \overbrace{\sqrt{\rho_{ul_k}}\sum_{i=1}^{K}\left(\boldsymbol{W}\hat{\boldsymbol{H}}_{ul}\right)_{k,i}\boldsymbol{x}_i}^{\text{Desired Signal+Interference}} + \boldsymbol{z}_k \tag{5}$$

where z_k is the amplified noise for user k caused by the decoder. The "Cumulative Error" part represents the interference introduced by CSI estimation inaccuracies. The "Desired Signal + Interference" part consists of the UL transmitted symbol from user k and the interference caused by the inter-user spatial correlation.

A. MATCH FILTER RECEIVER

MF is a low complexity operation where the decoder used in the equalization process can be written as $\boldsymbol{W} = \hat{\boldsymbol{H}}_{ul}^H$. The equalized signal vector can be written as follows:

$$\hat{\boldsymbol{x}}_k = \underbrace{\sqrt{\rho_{ul}}\sum_{i=1}^{K}\left(\hat{\boldsymbol{H}}_{ul}^H\boldsymbol{E}_{ul}\right)_{k,i}\boldsymbol{x}_i}_{\text{Cumulative Error}} + \overbrace{\sqrt{\rho_{ul}}\sum_{i=1}^{K}\left(\hat{\boldsymbol{H}}_{ul}^H\hat{\boldsymbol{H}}_{ul}\right)_{k,i}\boldsymbol{x}_i}^{\text{Desired Signal + Interference}} + \boldsymbol{z}_k \tag{6}$$

By increasing the number of antennas at the BS, the ratio between diagonal elements and non-diagonal elements of the Gram matrix $\boldsymbol{G} = \hat{\boldsymbol{H}}_{ul}^H\hat{\boldsymbol{H}}_{ul}$ will also increase. This is known as the channel hardening effect as previously mentioned [6]. The "Desired Signal + Interference" part is extremely sensitive upon the number of antennas at the BS. The "Cumulative Error" part is less impacted by the number of antennas since the matrix elements resulting from the matrix multiplication of $\left(\hat{\boldsymbol{H}}_{ul}^H\boldsymbol{E}_{ul}\right)$ are far smaller than the channel Gram matrix when UL power control is applied. The interference from both parts is increased by increasing the number of users.

B. ZERO FORCING RECEIVER

ZF tends to improve the performance by suppressing the interference between users and enhancing the number of simultaneous users. The decoder used in the equalization can be written as $\boldsymbol{W} = \left(\hat{\boldsymbol{H}}_{ul}^H\hat{\boldsymbol{H}}_{ul}\right)^{-1}\hat{\boldsymbol{H}}_{ul}^H$. The equalized signal vector can be written as follows:

$$\hat{\boldsymbol{x}}_k = \underbrace{\sqrt{\rho_{ul_k}}\sum_{i=1}^{K}\left(\left(\left(\hat{\boldsymbol{H}}_{ul}^H\hat{\boldsymbol{H}}_{ul}\right)^{-1}\hat{\boldsymbol{H}}_{ul}^H\boldsymbol{E}_{ul}\right)_{k,i}\boldsymbol{x}_i\right)}_{\text{Cumulative Error}} + \sqrt{\rho_{ul_k}}\boldsymbol{x}_i + \boldsymbol{z}_k \tag{7}$$

Unlike MF, the interference is only caused from the "Cumulative Error" part which is introduced by CSI estimation inaccuracies. This interference is increased by increasing number of users. Similar to MF, the channel Gram matrix impacts the interference value. Although ZF suppresses the interference from the estimated channel between users, it amplifies the interference introduced by the inaccurate CSI. This interference is caused by the inverse of the channel Gram matrix in the "Cumulative Error" part. Although the value of this part in ZF is larger than the one in MF, the overall interference in MF is still higher than that of ZF.

C. MINIMUM MEAN SQUARE ERROR RECEIVER

MMSE is a high complexity algorithm and enables the decoder to compromise between ZF and MF performance with low and high SNR respectively. The decoder used in the equalization process can be written as $\boldsymbol{W} = \left(\hat{\boldsymbol{H}}_{ul}^H\hat{\boldsymbol{H}}_{ul} + \frac{1}{\gamma}\boldsymbol{I}\right)^{-1}\hat{\boldsymbol{H}}_{ul}^H$, where γ is the SNR. The equalized signal vector can be written as follows:

$$\begin{aligned}\hat{\boldsymbol{x}}_k = &\overbrace{\sqrt{\rho_{ul_k}}\sum_{i=1}^{K}\left(\left(\left(\hat{\boldsymbol{H}}_{ul}^H\hat{\boldsymbol{H}}_{ul} + \frac{1}{\gamma}\boldsymbol{I}\right)^{-1}\hat{\boldsymbol{H}}_{ul}^H\boldsymbol{E}_{ul}\right)_{k,i}\boldsymbol{x}_i\right)}^{\text{Cumulative Error}} \\ &+ \underbrace{\sqrt{\rho_{ul}}\sum_{i=1}^{K}\left(\left(\hat{\boldsymbol{H}}_{ul}^H\hat{\boldsymbol{H}}_{ul} + \frac{1}{\gamma}\boldsymbol{I}\right)^{-1}\hat{\boldsymbol{H}}_{ul}^H\hat{\boldsymbol{H}}_{ul}\right)_{k,i}\boldsymbol{x}_i}_{\text{Desired Signal + Interference}} + \boldsymbol{z}_k\end{aligned} \tag{8}$$

The interference and the cumulative error parts are highly affected by the SNR value and the number of users. With a low SNR value, the MMSE performs similar to MF. While with a high SNR value, it performs similar to ZF.

V. IMPERFECT CHANNEL RECIPROCITY AND ACCUMULATIVE ERROR AMPLIFICATION IN DL

Channel reciprocity is essential for DL data transmission in a massive MIMO TDD system. Not only propagation conditions determine the radio channel, but also the transceiver front-ends at both sides of the radio link. Since different transceiver chains are used at the BS and the UE, the actual downlink channel $\boldsymbol{h}_{dl} \in \mathbb{C}^{1\times M}$ between the BS and one user can be written as follows:

$$\boldsymbol{h}_{dl} = \boldsymbol{h}_{ul}^{T}\boldsymbol{D}_b \tag{9}$$

Where $\boldsymbol{D}_b = diag\,(cb_1, ..., cb_M)$ is the calibration matrix and b_i is the calibration coefficient [15]. The estimated calibrated version of the downlink channel $\hat{\boldsymbol{h}}_{dl} \in \mathbb{C}^{1\times M}$ between one user and the BS can be written as follows:

$$\hat{\boldsymbol{h}}_{dl} = \hat{\boldsymbol{h}}_{ul}^{T}\hat{\boldsymbol{D}}_b \tag{10}$$

Where $\hat{\boldsymbol{D}}_b = diag\left(\hat{b}_1, ..., \hat{b}_M\right)$ is the estimated calibration matrix. $\hat{b}_i = c\,(b_i + e_i)$ is the estimated calibration coefficient where e_i is an IID random process representing the calibration error and c is the unknown common scaling factor. From (1), (9) and (10), the actual downlink channel $\boldsymbol{h}_{dl}$ between the BS and one user can be written as follows:

$$\begin{aligned}
\boldsymbol{h}_{dl} - \hat{\boldsymbol{h}}_{dl} &= \boldsymbol{h}_{ul}^{T}\boldsymbol{D}_b - \hat{\boldsymbol{h}}_{ul}^{T}\hat{\boldsymbol{D}}_b \\
\boldsymbol{h}_{dl} &= \hat{\boldsymbol{h}}_{dl} + \left(\hat{\boldsymbol{h}}_{ul}^{T} + \boldsymbol{e}_{ul}^{T}\right)\boldsymbol{D}_b - \hat{\boldsymbol{h}}_{ul}^{T}\hat{\boldsymbol{D}}_b \\
\boldsymbol{h}_{dl} &= \hat{\boldsymbol{h}}_{dl} + \hat{\boldsymbol{h}}_{ul}^{T}\left(\boldsymbol{D}_b - \hat{\boldsymbol{D}}_b\right) + \boldsymbol{e}_{ul}^{T}\boldsymbol{D}_b \\
\boldsymbol{h}_{dl} &= \hat{\boldsymbol{h}}_{dl} + \hat{\boldsymbol{h}}_{ul}^{T}\boldsymbol{E}_b + \boldsymbol{e}_{ul}^{T}\boldsymbol{D}_b \\
\boldsymbol{h}_{dl} &= \hat{\boldsymbol{h}}_{dl} + \boldsymbol{e}_{dl}
\end{aligned} \tag{11}$$

where

$$\boldsymbol{e}_{dl} = \hat{\boldsymbol{h}}_{ul}^{T}\boldsymbol{E}_b + \boldsymbol{e}_{ul}^{T}\boldsymbol{D}_b \tag{12}$$

$\boldsymbol{E}_b = diag\,(-ce_1, ..., -ce_M)$ is the calibration error matrix. From (11), the downlink channel matrix $\boldsymbol{H}_{dl} \in \mathbb{C}^{K\times M}$ between the BS and the UEs can be decomposed as follows:

$$\boldsymbol{H}_{dl} = \hat{\boldsymbol{H}}_{dl} + \boldsymbol{E}_{dl} \tag{13}$$

where $\hat{\boldsymbol{H}}_{dl} \in \mathbb{C}^{K\times M}$ is the estimated calibrated version of the downlink channel matrix between the UEs and the BS, while $\boldsymbol{E}_{dl} \in \mathbb{C}^{K\times M}$ is the difference between the estimated calibrated channel and the actual channel during the downlink transmission.

The UL CSI accuracy has greater impact on increasing the difference between the estimated calibrated channel and the actual channel during the downlink transmission than it has on increasing the difference between the estimated channel and the actual channel during the uplink data transmission. This can be seen in (12) where the error introduced by inaccurate UL CSI ($\boldsymbol{e}_{ul}$) is multiplied by the calibration matrix ($\boldsymbol{D}_b$). That means the difference between the estimated calibrated channel and the actual channel during the downlink transmission could vary with different massive MIMO hardware using the same reciprocity calibration algorithm and the same radio prorogation environment due to varying the hardware impairment. This was experimentally validated in section VIII. The hardware impairment error value in DL data transmission is greater than that in UL data transmission. This can be seen in equation (12) where the calibrated DL CSI error is composed from multiplying the UL CSI error to the calibration matrix then adding the multiplication result of the estimated UL CSI to the calibration error matrix. The received signal in DL can be written from (3) and (13) as follows:

$$\begin{aligned}
\hat{\boldsymbol{s}} &= \sqrt{\rho_{dl}}\boldsymbol{H}_{dl}\boldsymbol{P}\boldsymbol{s} + \boldsymbol{d} \\
&= \sqrt{\rho_{dl}}\left(\boldsymbol{E}_{dl}\boldsymbol{P} + \hat{\boldsymbol{H}}_{dl}\boldsymbol{P}\right)\boldsymbol{s} + \boldsymbol{d} \\
&= \sqrt{\rho_{dl}}\boldsymbol{E}_{dl}\boldsymbol{P}\boldsymbol{s} + \sqrt{\rho_{dl}}\hat{\boldsymbol{H}}_{dl}\boldsymbol{P}\boldsymbol{s} + \boldsymbol{d}
\end{aligned} \tag{14}$$

By rearranging the above equation, the received signal for user k can be written as follows:

$$\hat{\boldsymbol{s}}_k = \underbrace{\sqrt{\rho_{dl_k}}\sum_{i=1}^{K}\left(\boldsymbol{E}_{dl}\boldsymbol{P}\right)_{k,i}\boldsymbol{s}_i}_{\text{Cumulative Error}} + \overbrace{\sqrt{\rho_{dl_k}}\sum_{i=1}^{K}\left(\hat{\boldsymbol{H}}_{dl}\boldsymbol{P}\right)_{k,i}\boldsymbol{s}_i + \boldsymbol{d}_k}^{\text{Desired Signal+Interference}}$$

where

$$\boldsymbol{P} = \begin{cases} \hat{\boldsymbol{H}}_{dl} & MF \\ \left(\hat{\boldsymbol{H}}_{dl}\hat{\boldsymbol{H}}_{dl}^{H}\right)^{-1}\hat{\boldsymbol{H}}_{dl} & ZF \\ \left(\hat{\boldsymbol{H}}_{dl}\hat{\boldsymbol{H}}_{dl}^{H} + \frac{1}{\gamma}\boldsymbol{I}\right)^{-1}\hat{\boldsymbol{H}}_{dl} & MMSE \end{cases} \tag{15}$$

Since $\boldsymbol{E}_{dl} > \boldsymbol{E}_{ul}$, the interference caused by the "Cumulative Error" part in DL data transmission from equation (14) is greater than the one caused in UL data transmission from equation (4). Therefore, adding more users increases the interference between users in DL data transmission more than for UL data transmission. So the sum SE achieved in UL data transmission is greater than the one in DL data transmission. This was experimentally validated in section VIII.

VI. SPECTRAL EFFICIENCY EVALUATION

Two different scenarios were considered to evaluate the massive MIMO performance for differing numbers of users when CSI errors are present. An IID Rayleigh channel is used in the first scenario, where M = 128 and K is an even number $\in [2, 22]$. In the second scenario, the real channel captured from the trial described in section II was used. These scenarios were run through an UL massive MIMO simulator developed at the University of Bristol. In addition to randomly generated channels, new vectors can be transmitted through channels previously captured by the physical system for more extensive analysis. For both scenarios in this section, the error in the channel estimation between the UEs and the BS is modeled as a complex Gaussian distribution $\sim \mathcal{CN}\left(\boldsymbol{0}, \sigma_e^2\boldsymbol{I}_M\right)$ [18] where an error variance of 0.01 (1%) was used for the simulations shown. Whilst this value may be higher or lower and the model could not be so accurate in

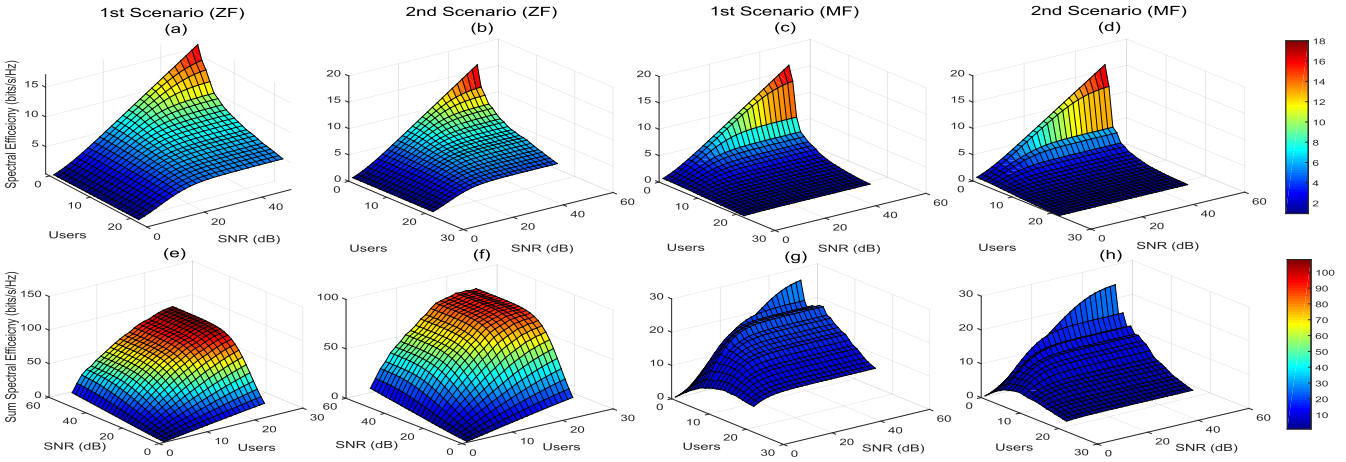

Fig. 3. SE (1st row) and sum SE (2nd row) comparison between iid Rayleigh channel and measured indoor channel with ZF and MF.

reality, it serves to illustrate the potential effects of CSI inaccuracies in massive MIMO. Simulation results with different error variance are covered in section VII while real-time results are covered in section VIII. The users were introduced in an order where the least overall correlation are considered first to minimize the inter-user interference (IUI) damage with each step.

A. THEORETICAL EVALUATION

Fig. 3 shows SE comparison between the 1st and the 2nd scenario as the number of active users increases across an SNR range of 0−50 dB for both ZF and MF algorithms. The sub-plots in the first row show the median achievable SE per user by using ZF and MF for both scenarios. Their equivalent sum SE are the sub-plots in the second row. The median per user SE is always 16.59 bits/s/Hz at 50 dB SNR in case of one active user since there is no interference source. For ZF it can be seen in (a) and (b) that a median per user spectral efficiency of greater than 4 bits/s/Hz can always be maintained at 30 dB SNR. Increasing the SNR beyond 30 dB improves lower numbers of active users, but plateaus at 4.89 bits/s/Hz in (a) and 4.219 bits/s/Hz in (b) for 22 users at 40 dB SNR. Sub-plot (e) and (f) in Fig. 3 show the sum SE for 1st and 2nd scenario respectively. With ZF, the median per user SE difference between 1st and 2nd scenario is small since the interference is only caused by the cumulative error part in (7) where the off-diagonal values of the Gram matrix for 1st scenario is less than those from 2nd scenario. Despite the small difference in per user SE, the maximum sum SE in 1st scenario outperform the one from 2nd scenario by 14.89 bits/s/Hz since 22 users are served simultaneously.

With MF, the median per user SE is greatly affected by adding more users as shown in Fig. 3, sub-plots (c) and (d). The maximum sum SE is achieved when only two users are selected in both scenarios. For 22 users, the sum SE in 1st scenario is greater by 6.98 bits/s/Hz at 50 dB SNR.

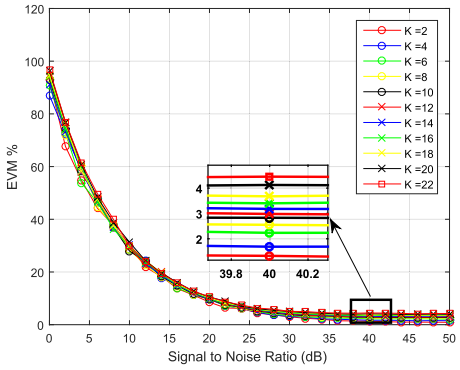

Fig. 4. EVM performance with ZF in iid Rayleigh channel.

B. PRACTICAL EVALUATION

A common measurement of signal quality used in 3GPP long-term evolution (LTE) standards is the EVM. It is a comprehensive metric which embraces all impairments on the transmitted signal as seen by the receiver.

Higher MCS are supported when the EVM is smaller [21]. From [21] and [22], the EVM can be given as

$$\mathrm{EVM}_k = \sqrt{\frac{\frac{1}{N}\sum_{n=1}^{N}|S_r(n)-S_t(n)|^2}{\frac{1}{N}\sum_{n=1}^{N}|S_t(n)|^2}} \times 100 \qquad (16)$$

where N is the number of symbols the EVM was measured over. $S_r(n)$ is the nth normalized received symbol and $S_t(n)$ is the ideal value of the nth symbol. For comprehensive analysis, the EVM was plotted for the 1st and the 2nd scenarios by using ZF and MF. Based on the 3GPP LTE standards, the required EVM for 64 QAM is 9% [21]. The required EVM to achieve 256 QAM is currently being considered and simulation campaigns shown it might be in the range of $1.5\% - 4\%$ [23].

Fig. 4 and Fig. 5 show the EVM results with ZF for the 1st and the 2nd scenarios respectively. For the 1st scenario,

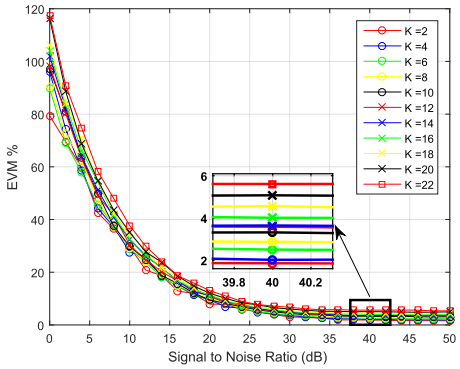

Fig. 5. EVM performance with ZF in measured indoor channel.

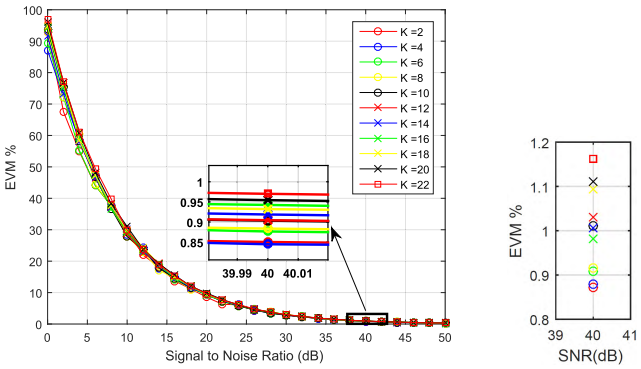

Fig. 6. EVM performance with ZF and perfect CSI. iid Rayleigh scenario in the left and measured indoor scenario at 40 dB SNR in the right.

TABLE 1. Realistic Performance (iid Rayleigh Scenario with ZF).

	Serving all Users		Maximizing Sum SE
K	22	25	19
MCS	64-QAM	64-QAM	256-QAM
Sum SE	72.864 b/s/Hz	82.8 b/s/Hz	83.9 b/s/Hz

TABLE 2. Realistic Performance (Measured indoor scenario with ZF).

	Serving all Users		Maximizing Sum SE
K	17	21	16
MCS	64-QAM	64-QAM	256-QAM
Sum SE	56.3 b/s/Hz	69.55 b/s/Hz	70.656 b/s/Hz

Fig. 7. Impact of user number on the observed EVM. 64-QAM with ZF for 24 users on the left and 22 users on the right.

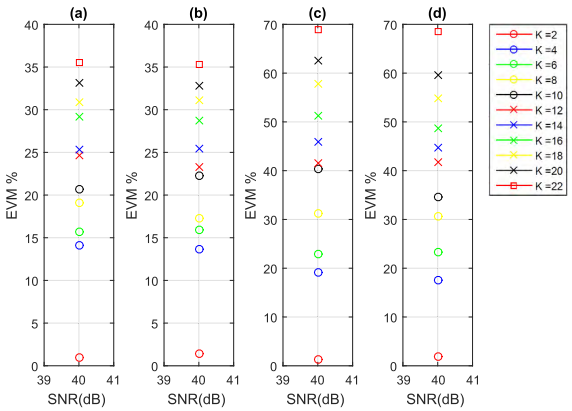

Fig. 8. EVM performance comparison with MF between 1st (a&b) and 2nd (c&d) scenario.

the EVM range was between 1.5% and 4.5% which corresponds to K from 2 till 22 with 40 dB SNR. In the 2nd scenario, the EVM performance was slightly degraded and its range becomes between 1.9% and 5.8%. The increment in the EVM range is caused by the high spatial correlation in the 2nd scenario which amplifies the impact of inaccurate CSI. Table 1 and Table 2 show the sum SE results at 40 dB SNR for the 1st and 2nd scenarios respectively. In the 1st scenario, the maximum sum SE is achieved by serving 19 users simultaneously with 256-QAM.

When adding more users, 64-QAM is used in order to provide reliable communications. Here the SE will only be increased when 26 or more users are served. In the 2nd scenario, the maximum sum SE is achieved by serving 16 users simultaneously with 256-QAM. This value can only be increased by adding more than five users if 64-QAM is applied. As it is shown in both scenarios, by adding more users the EVM performance becomes worse and the sum SE could be decreased. The degradation in the EVM performance can be seen in Fig. 7, which shows a realistic 64-QAM constellations captured from the trial in [24]. The constellations on the left were captured with 24 active users.

The constellations on the right were captured after removing two users randomly. The observed EVM was enhanced just by removing two users since the ''Cumulative Error'' part in (7) was reduced by two users. The EVM performance with perfect CSI is shown in Fig. 6 where the left plot is for the 1st scenario and the right plot is for the 2nd scenario. The EVM performance was enhanced and its range lies between 0.85% and 0.97% in 1st scenario and between 0.89% and 1.18% in 2nd scenario which corresponds to K from 2 till 22 with 40 dB SNR. With perfect CSI, the EVM performance is slightly affected by the number of users since it only amplifies the noise. Fig. 8 shows the EVM results with MF for 1st and 2nd scenarios with 40 dB SNR. The sub-plot a and b are for the 1st scenario with perfect and inaccurate CSI respectively. The sub-plot c and d are for the 2nd scenario with perfect and inaccurate CSI respectively. The impact of inaccurate CSI can be ignored in both scenarios. The EVM performance is highly affected by the number of users. Compared to ZF, the EVM value corresponds to 22 users is increased by 30.5% in the 1st scenario and 64% in the 2nd scenario. In the 1st scenario, the maximum number of users that can be served is 8 using quadrature phase-shift keying (QPSK). In the second

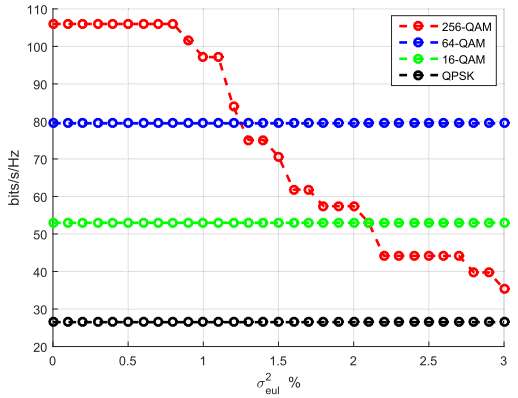

Fig. 9. Maximum sum SE with ZF and MMSE in UL by different MCS.

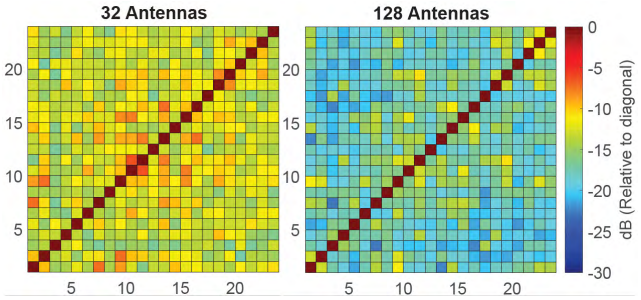

Fig. 10. User-side Gramian intensity plots for 24 UEs for the measured indoor scenario.

scenario, the maximum number of users is reduced by two using the same MCS. Maximum sum SE of 8.832 bits/s/Hz is achieved by serving two users with 256-QAM in both scenarios.

VII. NUMBER OF ANTENNAS AT BS COMPARED TO HARDWARE QUALITY

By further inspecting the results obtained in section II and applying the practical evaluation method in section VI-B, some insight can be gained on the trend of maximizing the sum SE with the relation to the number of BS antennas, spatial correlation between users and CSI accuracy. Fig. 10 shows the intensity plot results for the user-side Gramian matrix for 32 and 128 elements of the 4×32 patch array. For the 32 antenna case, the results were obtained using the second 4×8 panel in from the left when facing the array. The first thing that can be seen is that the correlation level between UEs with 128 BS antennas is lower than the one with only 32 BS antennas due to the channel hardening effect. By using ZF and MMSE decoders in the UL massive MIMO simulator mentioned earlier with rate 3/4 low-density parity-check (LDPC) code as described in [25], the sum SE that can be achieved with each MCS and $\sigma^2_{e_{ul}} \in [0, 3\%]$ can be seen in Fig. 9. An IID Rayleigh channel is used, where M = 128 and K = 24. The maximum sum SE is achieved by serving all the 24 UEs with 256-QAM when $\sigma^2_{e_{ul}} \in [0, 0.8\%]$. When the UL error variance value is greater than 0.8%, the sum

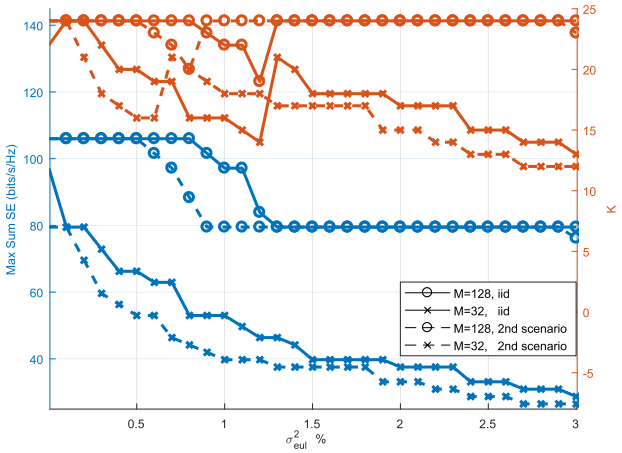

Fig. 11. Maximizing sum SE with ZF and MMSE in UL. Blue: maximum sum SE. Red: number of simultaneous users.

SE starts decreasing due to the lower number of UEs that can be served simultaneously in order to fulfill the EVM requirements for the 256-QAM. When $\sigma^2_{e_{ul}} \in [1.3\%, 3\%]$, the maximum sum SE is achieved by serving all the 24 UEs with 64-QAM. The blue color shows the maximum sum SE that can be achieved by using ZF or MMSE in Fig. 11 and MF in Fig. 12. For comparison purposes, the correspondent number of UEs have been plotted in red color on a second axis. Lower MCS order is being used each time the number of UEs is increased by increasing the value of $\sigma^2_{e_{ul}}$. An IID Rayleigh channel is used for the 1^{st} scenario, where K = 24 and M = 128. Then the number of antennas at the BS was decreased to 32 to increase the spatial correlation value between users. Both real-channels used to produce the results in Fig. 10 were used in the 2^{nd} scenario. With perfect CSI, 256-QAM is used in both scenarios with M = 128 and M = 32 in Fig. 11. When M = 128 and $\sigma^2_{e_{ul}} \in [0, 0.5\%]$, the maximum sum SE with the real-channel in the 2^{nd} scenario was similar to the one achieved by the IID channel where 24 UEs are served simultaneously. When $\sigma^2_{e_{ul}} \in [0.6\%, 0.8\%]$ and $\sigma^2_{e_{ul}} \in [0.9\%, 1.2\%]$, number of UEs is decreased for the real-channel and IID channel respectively in order to fulfill the 256-QAM requirements. But when $\sigma^2_{e_{ul}} \geq 0.9\%$ and $\sigma^2_{e_{ul}} \geq 1.3\%$, the maximum sum SE is achieved by serving all the 24 UEs with 64QAM except when $\sigma^2_{e_{ul}} = 3$ with the real-channel scenario. By decreasing number of antennas at the BS to 32, the maximum sum SE become more sensitive to the accuracy of CSI. The maximum sum SE dropped by 58 bit/s/Hz when $\sigma^2_{e_{ul}}$ is increased from 0 to 3% with real-channel in 2^{nd} scenario. While it was only decreased by 34 bit/s/Hz with 128 antennas at the BS. Besides, the same maximum sum SE is achieved by using real-channel or IID channel with most of the CSI accuracy when M = 128. While the maximum sum SE is always achieved by using IID channel when M = 32.

These results can be explained from the "Cumulative Error" part in (7) and (8). When M = 128, the matrix elements resulting from inverting the Gram matrix $\left(\hat{\boldsymbol{H}}^H_{ul}\hat{\boldsymbol{H}}_{ul}\right)^{-1}$

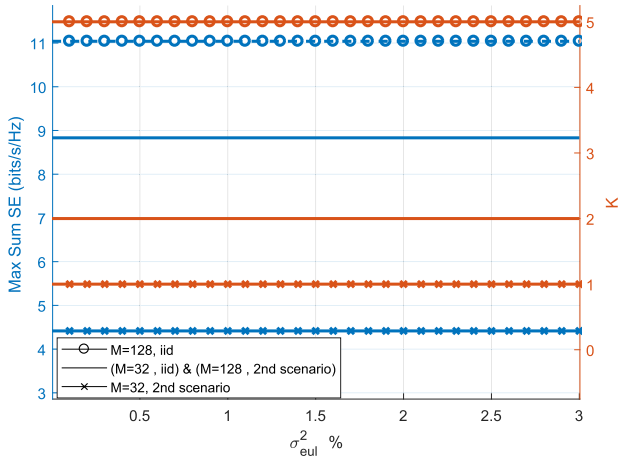

Fig. 12. Maximizing sum SE with MF in UL. Blue: maximum sum SE. Red: number of simultaneous users.

are small because of the channel hardening effect. Therefore, the interference resulting in this part will be small as well and more UEs can be served simultaneously with higher MCS. While when M = 32, the matrix elements resulting from inverting the Gram matrix $\left(\hat{\boldsymbol{H}}_{ul}^{H}\hat{\boldsymbol{H}}_{ul}\right)^{-1}$ are high. Therefore lower MCS with less number of UEs are used.

When MF decoder is used, the maximum sum SE is not affected with the CSI accuracy when $\sigma^2_{e_{ul}} \in [0, 3\%]$ as it is shown in Fig. 12. The maximum sum SE is achieved by serving five UEs with 16-QAM using an IID channel with M = 128. While by using the same number of antennas with real-channel, the maximum sum SE is decreased by 2.1 bits/s/Hz which is the same results obtained from 32 antennas with an IID channel. This is achieved by serving two UEs with 256-QAM. The lowest maximum sum SE is achieved by serving only one user with 256-QAM using real-channel with M = 32. Although MF decoder has very low sensitivity to CSI accuracy, it is highly sensitive to number of antennas and spatial correlation values between UEs.

Increasing number of antennas at the BS could be expensive because of the additional hardware requirements. Massive MIMO with high CSI accuracy and low number of antennas could be a better investment if it costs less and has similar performance. This can be achieved by using hardware with high quality to reduce the hardware impairment error and the noise floor value. Fig. 11 shows that with 32 antennas at the BS and $\sigma^2_{e_{ul}} = 0.1\%$, the same maximum sum SE can be achieved when number of antennas is increased to 128 with $\sigma^2_{e_{ul}} \geq 0.9\%$. This was experimentally validated in the next section.

VIII. REAL-TIME EVALUATION USING MASSIVE MIMO TEST-BED

In this section, we present real-time results from the massive MIMO testbed in [26]. These results demonstrate the impact of inaccurate CSI on the SE and show that increasing number

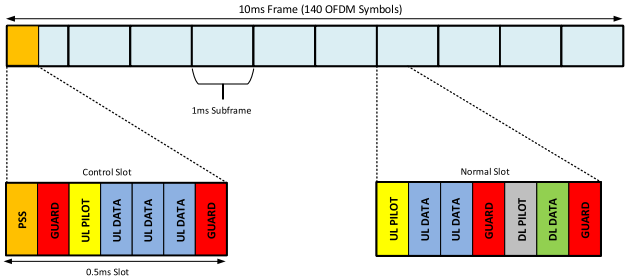

Fig. 13. Frame Schedule.

of antennas at the BS can decrease this impact. It also validates the following:

- The maximum sum SE with practical number of antennas could be achieved by decreasing the number of users.
- Inaccurate UL CSI has greater impact on the DL data transmission than it has on the UL data transmission due to the error amplification caused by the reciprocity calibration matrix.
- By using ZF or MMSE, a lower number of antennas at the BS with high hardware quality could be better than increasing number of antennas and reducing the hardware quality.

MF, ZF and MMSE were used for UL and DL data transmission by using the exact same static environment but with two different UL CSI accuracy values.

A. FRAME SCHEDULE

The PHY frame schedule used for the system is shown in Fig. 13. In its default configuration, it is based closely upon the TD-LTE standard, but it can be completely customized at the Orthogonal Frequency Division Multiplexing (OFDM) symbol level to allow a range of configurations to be applied for different applications. For the SE results shown in this section, two different frame schedules were configured for two different scenarios. For the UL scenario, only UL data with two UL pilots per radio frame were used. While in the DL scenario, only DL data with two UL pilots and two DL pilots per radio frame were used. The first OFDM subframe is for synchronization in both scenarios to achieve sample alignment.

B. LOW CSI ACCURACY

For low CSI accuracy, over-the-air (OTA) synchronization was used based on Zadoff-Chu sequence. The phase of the sync signal was generated randomly from each antenna at the BS which created nulls in different locations. This caused sync losses for the users based on their locations and the sync signal phases from the antennas at the BS. The synchronization error causes Inter-Carrier Interference (ICI), Inter-Symbol Interference (ISI) and interference between data streams due to the inaccurate CSI. The BS and the users save the sequence number of each transmitted radio frame. When the user doesn't detect the sync signal, it saves the radio frame number. The sum SE calculation doesn't consider the data

Fig. 14. Measurement Environment.

transmission between the user who lost the sync signal and the BS. This can be done by removing the data transmitted during saved radio frame number in both UL and DL for that user. By doing that, the impact of ICI and ISI was removed before calculating the sum SE while the interference caused by the inaccurate CSI is only considered in this scenario.

C. HIGH CSI ACCURACY

To increase the CSI accuracy, cabled synchronization was used with an Octoclock module [27]. To achieve sample alignment, a start trigger that signals the start of the first radio frame is fanned out to all radios by equal length cables. The user clients were connected to the Octoclock by extended cable and the timing offsets were corrected for. For fair comparison, when the data transmitted between the UE and the BS was removed from the sum SE calculation in the low CSI accuracy scenario, it was also removed from the high CSI accuracy scenario.

D. MEASUREMENT ENVIRONMENT

The Communication Systems & Networks (CSN) lab was used for LOS measurements between the BS and 12 UEs from 6 universal software radio peripheral (USRP)s. Measurements were performed outside of university hours and the massive MIMO test-bed was controlled remotely to ensure the same static environment was applied in all scenarios. An overview of the setup can be seen in Fig. 14. At the BS side, 64 element array was used providing half-wavelength spacing at 3.5 GHz. A floor plan of the experiment is shown in Fig. 15 with the UE locations.

E. VALIDATION RESULTS

Table 3 and Table 4 show the maximum uncoded sum SE results for the UL scenario with high and low CSI accuracy respectively. Maximum sum SE of 56.59 bits/s/Hz is achieved by using ZF or MMSE with M = 64 and high CSI accuracy serving all the 12 UEs with 64-QAM. Although no error correction was used, this value is equal to the error free version using the same frame schedule, number of UEs and MCS. By reducing the number of antennas to 32, the maximum sum SE is decreased by 6.39 bits/s/Hz due to the

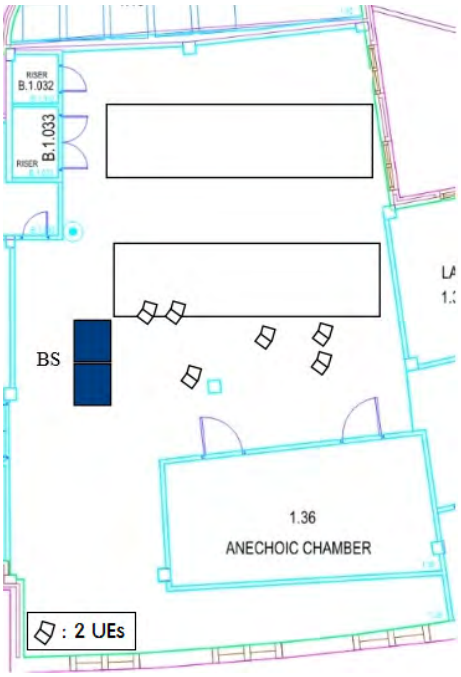

Fig. 15. CSN Lab floor plan showing the BS and UEs locations.

TABLE 3. Trial Results for UL Scenario (High CSI Accuracy).

	K / MCS		Sum SE (b/s/Hz)	
	M=32	M=64	M=32	M=64
MF	K=3, b=2	K=2, b=4	4.4	6.2
ZF& MMSE	K=12, b=6	K=12, b=6	50.2	56.59

higher interference level although the same number of UEs and MCS are used. The interference caused by "Cumulative Error" part in (7) and (8) when M = 64 is less than the one when M = 32 due to the channel hardening effect. With low CSI accuracy, the maximum sum SE with ZF or MMSE is decreased by 7.49 bits/s/Hz and 13.2 bits/s/Hz for M = 64 and M = 32 respectively. Decreasing the CSI accuracy has greater impact when M = 32 with ZF and MMSE. These results validate the theoretical work on massive MIMO showing that by increasing number of antennas at the BS, the interference caused by inaccurate CSI with ZF and MMSE will decrease. With MF, the CSI accuracy has no impact on the maximum sum SE. Only the number of antennas affect the maximum sum SE achieved by MF in the UL scenario. This can be explained from (6) where the interference caused by the "Desired Signal + Interference" part, that is sensitive upon the number of antennas, is very large compared to the one caused by the "Cumulative Error" part which is affected by the CSI accuracy.

Table 5 and Table 6 show the maximum uncoded sum SE results for the DL scenario with high and low CSI accuracy respectively. The maximum sum SE results are decreased in the DL scenario due to the difference between the estimated calibrated channel and the actual channel during DL transmission. With high CSI accuracy and

TABLE 4. Trial Results for UL Scenario (Low CSI Accuracy).

	K / MCS		Sum SE (b/s/Hz)	
	M=32	M=64	M=32	M=64
MF	K=3, b=2	K=2, b=4	4.4	6.2
ZF& MMSE	K=9, b=6	K=11, b=6	37	49.1

TABLE 5. Trial Results for DL Scenario (High CSI Accuracy).

	K / MCS		Sum SE (b/s/Hz)	
	M=32	M=64	M=32	M=64
MF	K=3, b=2	K=3, b=2	3.8	4.5
ZF& MMSE	K=10, b=4	K=11, b=4	31	34.4

TABLE 6. Trial Results for DL Scenario (Low CSI Accuracy).

	MCS / K		Sum SE (b/s/Hz)	
	M=32	M=64	M=32	M=64
MF	K=3, b=2	K=2, b=4	3.2	4.2
ZF& MMSE	K=6, b=2	K=10, b=2	8	15

ZF or MMSE precoders, the maximum sum SE is decreased by 22.19 bits/s/Hz and 19.2 bits/s/Hz with $M = 64$ and $M = 32$ respectively compared to the UL scenario with high CSI accuracy. While by applying the same comparison for the low CSI accuracy, the maximum sum SE is decreased by 34.1 bits/s/Hz and 29 bits/s/Hz with $M = 64$ and $M = 32$ respectively. By comparing the SE degradation between UL and DL scenarios with high and low CSI accuracy, the maximum sum SE with low CSI accuracy was shown to be affected more. The additional maximum sum SE degradation due to low CSI accuracy was 11.91 bits/s/Hz and 9.81 bits/s/Hz with $M = 64$ and $M = 32$ respectively, despite using the same reciprocity calibration algorithm. This can be explained in (12) where the error introduced by inaccurate UL CSI ($\boldsymbol{e}_{ul}$) is multiplied by the calibration matrix ($\boldsymbol{D}_b$). These results validate that UL CSI accuracy has greater impact on the DL data transmission than it has on the UL data transmission.

By comparing the results between high CSI accuracy and low CSI accuracy in UL and DL scenarios, we can see that the maximum sum SE with 32 antennas and high CSI accuracy always outperforms the one from 64 antennas with low CSI accuracy when ZF or MMSE is used. This validates the simulation results in section VII and concludes that increasing number of antennas at the BS might not be efficient as much as increasing the hardware quality to acquire more accurate CSI.

By serving all the 12 UEs, the maximum sum SE was only achieved in the UL scenario with ZF and MMSE using high CSI accuracy. While to achieve the maximum sum SE for the remaining scenarios, the number of UEs was decreased. These results validate that the maximum sum SE with practical number of antennas could be achieved by decreasing number of users. From the results obtained in this section and section VII using ZF and MMSE, the maximum sum SE and number of UEs keep changing. That should emphasize the need for a user grouping algorithm not only at the cell edges, but also within the cell itself in order to maximize the sum SE.

IX. CONCLUSIONS

In this paper, the highest SE of 145.6 bits/s/Hz achieved for any wireless system to date and its limiting factors were presented. We have illustrated and experimentally validated the impact of the user number upon maximizing sum SE in a TDD single-cell massive MIMO system. Common linear decoders/precoders, MF, ZF and MMSE, were used in UL and DL data transmission cases. A practical method based on EVM performance for realistic SE calculation was compared with the theoretical method based on Shannon capacity. By using both IID Rayleigh and measured massive MIMO channels with 1% CSI estimation error, it was shown that the maximum theoretical sum SE is achieved by increasing the number of users. Unlike the conventional method for theoretical SE calculation or assuming perfect CSI, it was shown and experimentally validated that the maximum sum SE could be achieved by decreasing the number of users with practical number of antennas at the BS.

Furthermore, It was shown and experimentally validated that the inaccurate UL CSI has greater impact on the DL data transmission than it was on the UL data transmission due to the reciprocity calibration error amplification. Besides, by using ZF or MMSE, a lower number of antennas at the BS with high hardware quality could be better than increasing the number of antennas and reducing the hardware quality.

ACKNOWLEDGMENT

The authors wish to thank Bristol City Council for access to the hardware facility.

REFERENCES

[1] T. L. Marzetta, "Noncooperative cellular wireless with unlimited numbers of base station antennas," *IEEE Trans. Wireless Commun.*, vol. 9, no. 11, pp. 3590–3600, Nov. 2010.
[2] J. Hoydis, S. ten Brink, and M. Debbah, "Massive MIMO in the UL/DL of cellular networks: How many antennas do we need?" *IEEE J. Sel. Areas Commun.*, vol. 31, no. 2, pp. 160–171, Feb. 2013.
[3] W. Zhang *et al.*, "Field trial and future enhancements for TDD massive MIMO networks," in *Proc. 26th Annu. Int. Symp. Pers., Indoor, Mobile Radio Commun. (PIMRC)*, vol. 7, Aug./Sep. 2015, pp. 2339–2343.
[4] (2017). *Vodafone to Deploy 4G Massive MIMO in 2018*. [Online]. Available: https://zd.net/2MjwvKw
[5] (2016). *Facebook Project Aries*. [Online]. Available: https://bit.ly/2OxY5jQ
[6] T. L. Narasimhan and A. Chockalingam, "Channel hardening-exploiting message passing (CHEMP) receiver in large-scale MIMO systems," *IEEE J. Sel. Topics Signal Process.*, vol. 8, no. 5, pp. 847–860, Oct. 2014.
[7] P. Harris *et al.*, "LOS throughput measurements in real-time with a 128-antenna massive MIMO testbed," in *Proc. IEEE Global Commun. Conf. (GLOBECOM)*, Dec. 2016, pp. 1–7.
[8] P. Harris *et al.*, "Serving 22 users in real-time with a 128-antenna massive MIMO testbed," in *Proc. IEEE Int. Workshop Signal Process. Syst. (SiPS)*, Oct. 2016, pp. 266–272.
[9] W. B. Hasan, P. Harris, A. Doufexi, and M. Beach, "Spatial uplink power control for massive MIMO," in *Proc. IEEE 85th Veh. Technol. Conf. (VTC Spring)*, Jun. 2017, pp. 1–6.
[10] E. Björnson, E. G. Larsson, and T. L. Marzetta, "Massive MIMO: Ten myths and one critical question," *IEEE Commun. Mag.*, vol. 54, no. 2, pp. 114–123, Feb. 2016.

[11] U. Gustavsson *et al.*, "On the impact of hardware impairments on massive MIMO," in *Proc. IEEE Globecom Workshops (GC Wkshps)*, Dec. 2014, pp. 294–300.
[12] F. Athley, G. Durisi, and U. Gustavsson, "Analysis of massive MIMO with hardware impairments and different channel models," in *Proc. 9th Eur. Conf. Antennas Propag. (EUCAP)*, Apr. 2015, pp. 1–5.
[13] D. Mi, M. Dianati, L. Zhang, S. Muhaidat, and R. Tafazolli, "Massive MIMO performance with imperfect channel reciprocity and channel estimation error," *IEEE Trans. Commun.*, vol. 65, no. 9, pp. 3734–3749, Sep. 2017.
[14] T. L. Marzetta, E. G. Larsson, H. Yang, and H. Q. Ngo, *Fundamentals of Massive MIMO*. Cambridge, U.K.: Cambridge Univ. Press, 2016.
[15] E. Björnson, J. Hoydis, M. Kountouris, and M. Debbah, "Massive MIMO systems with non-ideal hardware: Energy efficiency, estimation, and capacity limits," *IEEE Trans. Inf. Theory*, vol. 60, no. 11, pp. 7112–7139, Nov. 2014.
[16] E. Björnson, E. G. Larsson, and M. Debbah, "Massive MIMO for maximal spectral efficiency: How many users and pilots should be allocated?" *IEEE Trans. Wireless Commun.*, vol. 15, no. 2, pp. 1293–1308, Feb. 2016.
[17] (2016). *5G Researchers Set New World Record For Spectrum Efficiency*. [Online]. Available: https://bit.ly/2LdO5KA
[18] S. Wagner, R. Couillet, M. Debbah, and D. T. M. Slock, "Large system analysis of linear precoding in correlated MISO broadcast channels under limited feedback," *IEEE Trans. Inf. Theory*, vol. 58, no. 7, pp. 4509–4537, Jul. 2012.
[19] C. A. Balanis, *Antenna Theory: Analysis and Design*. Hoboken, NJ, USA: Wiley, 2005.
[20] F. Kaltenberger, H. Jiang, M. Guillaud, and R. Knopp, "Relative channel reciprocity calibration in MIMO/TDD systems," in *Proc. IEEE Future Netw. Mobile Summit*, Jun. 2010, pp. 1–10.
[21] M. A. Finlayson, *LTE; Evolved Universal Terrestrial Radio Access (E-UTRA); Base Station (BS) Conformance Testing*, document TS 36.141 Version 10.1.0 Release 10, 3GPP, 2011.
[22] H. A. Mahmoud and H. Arslan, "Error vector magnitude to SNR conversion for nondata-aided receivers," *IEEE Trans. Wireless Commun.*, vol. 8, no. 5, pp. 2694–2704, May 2009.
[23] M. A. Finlayson, "LTE- advanced (3GPP Rel.12) technology introduction," 3GPP, Munich, Germany, White Paper 1MA252_1E, 2014.
[24] (2017). *Bristol and BT Collaborate on Massive MIMO Trials for 5G Wireless*. [Online]. Available: https://goo.gl/RpFdop
[25] S. Nowak and R. Kays, "An interleaving scheme for efficient binary LDPC coded higher-order modulation," in *Proc. Int. ITG Conf. Source Channel Coding (SCC)*, Jan. 2010, pp. 1–6.
[26] (2014). *Bristol Is Open*. [Online]. Available: http://www.bristolisopen.com
[27] (2014). Octoclock Specheet. [Online]. Available: http://www.ni.com/datasheet/pdf/en/ds-572

WAEL BOUKLEY HASAN received the M.Sc. degree (Hons.) in mobile communications engineering from Heriot-Watt University in 2013. He was with the Small Cells Platform Development Department, Alcatel-Lucent, for one year. He then joined the CDT in Communications, University of Bristol, in 2014. His research within the CSN Group is focused on investigating and developing different techniques for massive MIMO, with an interest in increasing spectral efficiency and power efficiency. He led the Massive MIMO Team at the 5G Layered Realities Weekend—Showcase in Bristol, successfully establishing reliable video streams in the world's first urban 5G showcase in 2018. He was also a member of the University of Bristol's Research Team that set spectral efficiency world records in 2016 in collaboration with the Lund University's Research Team.

PAUL HARRIS received the B.Eng. degree (Hons.) in electronic engineering from the University of Portsmouth in 2013 and the Ph.D. degree in communications from the University of Bristol in 2018. While completing the Ph.D. degree within the Communication Systems and Networks Group, University of Bristol, he was involved in collaboration with Lund University and National Instruments to implement a 128-antenna massive MIMO test system and led two research teams to set spectral efficiency world records in 2016. For this achievement, he received five international awards from National Instruments, Xilinx, and Hewlett Packard Enterprise, and an honorary mention in the 2016 IEEE ComSoc Student Competition for Communications Technology Changing the World. He is currently a Senior Systems Engineer and a Massive MIMO Platform Architect at Cohere Technologies.

ANGELA DOUFEXI received the B.Sc. degree in physics from the University of Athens, Greece, in 1996, the M.Sc. degree in electronic engineering from Cardiff University, Cardiff, U.K., in 1998, and the Ph.D. degree from the University of Bristol, U.K., in 2002. She is currently a Professor of wireless networks with the University of Bristol. Her research interests include vehicular communications, new waveforms, resource allocation, massive MIMO and multiple antenna systems, long-term evolution, mm-wave communications, and fifth-generation communications systems. She has authored over 200 journal and conference papers in these areas.

MARK BEACH is currently a Full Professor with the University of Bristol, U.K. He also manages the delivery of the CDT in Communications and leads research in the field of enabling technologies for the delivery of 5G and beyond wireless connectivity, as well as his role as the School Research Impact Director. He has over 25 years of physical layer wireless research embracing the application of spread spectrum technology for cellular systems, adaptive or smart antenna for capacity and range extension in wireless networks, MIMO-aided connectivity for throughput and spectrum efficiency enhancement, and millimeter-wave technologies and flexible RF technologies for SDR modems.